23rd ABCM International Congress of Mechanical Engineering
December 6-11, 2015, Rio de Janeiro, RJ, Brazil

NUMERICAL STUDY OF THE VORTEX-INDUCED VIBRATIONS OF AN ELASTIC CIRCULAR CYLINDER WITH 1 DEGREE OF FREEDOM USING OPENFOAM

Jose M. P. Conde
Ricardo M. V. Lopes
Unidemi, Faculdade de Ciências e Tecnologia, Universidade Nova de Lisboa
2829-516 Caparica, Portugal
jpc@fct.unl.pt, rmv.lopes@campus.fct.unl.pt

Abstract. *This paper presents a validation of the numerical code OpenFoam to problems with the vortex-induced vibration (VIV) phenomenon. This code was applied to the uniform flow past a circular cylinder that is allowed to move with 1 degree of freedom in the transverse direction to the flow. Firstly the flow around a fixed cylinder is simulated, and then is simulated a flow around an elastic cylinder. The Reynolds number is 200 for all simulations and the cylinder motion is described according to a mass-spring or a mass-spring-damper systems. The simulations were performed by solving the 2D Navier-Stokes equations. In the simulation of the flow around the fixed cylinder, the drag and lift coefficients and Strouhal number, were calculated and compared with results from other authors. The results obtained are similar those of other authors, however it was noticed that the discretization and domain size are very important for the accuracy of the results. In the simulations of the flow around the elastic cylinder (mass-spring or mass-spring-damper systems), drag and lift coefficients and the cylinder displacement were calculated. The results obtained in this study were satisfactory and it is concluded that the OpenFoam code is a reliable tool to solve problems with the VIV phenomenon.*

Keywords: *Elastic cylinder, Vortex-induced vibration, Navier-Stokes, OpenFoam.*

1. INTRODUCTION

Fluid-Structure interactions occur in many fields of engineering. The Vortex-Induced Vibration (VIV) phenomenon caused by the vortex shedding from a cylinder is an example of such interaction. The periodic force, generated by the periodic vortex shedding, causes the cylinder to vibrate, and at the same time, the oscillating cylinder will affect the fluid flow around itself and, as a consequence, the force and the vortex sheading pattern are affected.

Although the flow past cylinders, static or under VIV, have been already discussed in many papers and books (*e.g.*, Sumer and Fredsϕe, 1997; Zdravkovich, 1997; Blevins, 1977; Williamson and Govardhan, 2004), it is still a good test case for the validation of numerical codes.

The response of an elastic circular cylinder with one degree of freedom (1DOF) is influenced and characterized by a set of dimensionless variables (*e. g.*, Sumer and Fredsϕe, 1997):

- The Reynolds number, $Re = \rho U_\infty D/\mu$, where ρ is the fluid density, U_∞ is the free-stream velocity, and D is the cylinder diameter;
- The Strouhal number, $St = f_s D/U_\infty$, where f_s is the vortex-shedding frequency;
- The mass ratio, $m^* = 4m/\left(\pi\rho l D^2\right)$, where m and l are the cylinder mass and length, respectively, this parameter relates the cylinder average density with the fluid density, typically, small values of m^* can be related to fluid-structure interaction in water and large values in air;
- The reduced velocity, $U^* = U_\infty/\left(f_n D\right)$, where f_n is the natural frequency of the cylinder, $f_n = \sqrt{k/m}/\left(2\pi\right)$, and k is the spring stiffness constant;
- The damping ratio, $\zeta = c/\left(2\sqrt{mk}\right)$, where c is the damping coefficient;
- The combined mass-damping parameter, $m^*\zeta$;
- The stability parameter, $K_S = \pi^2 m^* \zeta$.

This paper starts by presenting a brief description of the numerical code OpenFOAM, the algorithms used, the mesh characteristics and the simulation conditions. To establish a baseline for comparison, firstly the flow past a fixed cylinder is simulated at Re=200 in 2D. Although for this value of Re the flow already presents some 3D characteristics, this is still a test case used by many authors (*e. g.*, Li *et al.*, 2009, Zhou *et al.*, 1999). Then is simulated a flow past a cylinder that is allow to move with 1 degree of freedom in the transverse direction to the flow.

2. NUMERICAL MODEL

The numerical code used in the work presented in this paper is the OpenFOAM version 2.2.2 (OpenFOAM, 2013). Two solvers were used: pimpleFoam and pimpleDyMFoam. Both use the PIMPLE algorithm, which is a combination of the classical SIMPLE and PISO. The first is used with static meshes while the second is used with movable meshes.

The numerical model solves the Navier-Stokes equations considering laminar flow, *i. e.*, without turbulence models. Only 2D simulations were performed. The motion of the cylinder is imposed by the equation of motion for 1DOF in the transverse direction of the flow:

$$m\ddot{y} + c\dot{y} + ky = F_y \tag{1}$$

where: y, $\dot{y}$, and $\ddot{y}$ are the displacement, the velocity and the acceleration, respectively; and F_y is the transverse force, *i. e.*, the lift force. This equation is applied by the solver sixDoFRigidDisplacement. The mesh reconstruction is achieved by the dynamicMotionSolverFvMesh solver. These solvers have been validated by Jasak and Tukovic (2010).

2.1 Computational domain and discretization mesh

For all the simulations presented in this paper one O-type mesh was used. Figure 1a presents the mesh for the entire domain. The domain is circular with its center coincident with the cylinder axis and the external radius, L_{ext}, is 50*D*. The cylinder diameter, *D*, is 1 m. Figure 1b presents a detail of the mesh in the proximity of the cylinder.

The mesh was generated using the code Gmsh (Geuzaine and Remacle, 2009). The distance of the first finite volume to the cylinder surface is 0.003*D*. The cylinder surface is discretized by 300 segments. The total of finite volumes in the mesh is 30000.

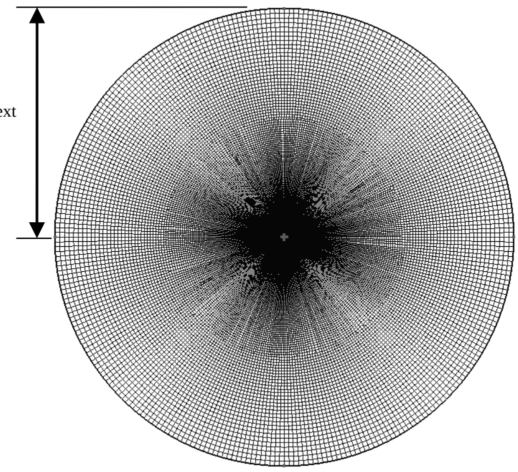

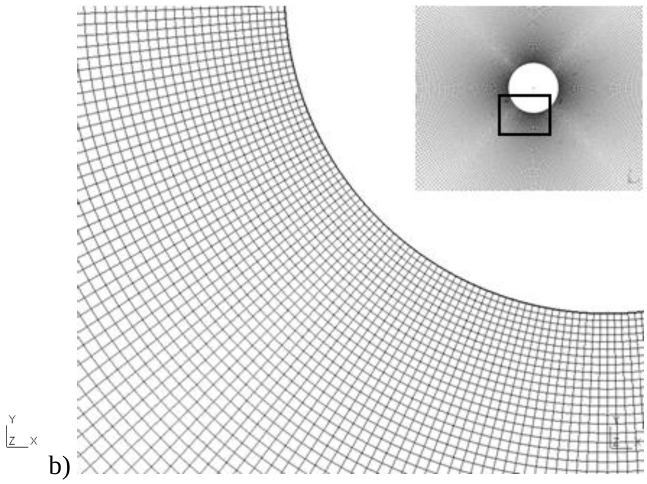

Figure 1. Computational domain and discretization mesh (a); mesh detail near the cylinder (b).

2.2 Simulation conditions

For all the simulations considered in this paper the Reynolds number is 200 and the mass ratio is 1.27. The values of the different variables imposed are: D = 1 m; ρ = 1 kg m^{-3}; μ = 0.005 kg m^{-1} s^{-1}; U_∞ = 1 m s^{-1}; m = 1 kg; l = 1 m.

The left half of the external circumference of the mesh (Fig. 1a) is used as inlet boundary and the right half as outflow boundary. At the inlet is imposed the fixed value of the undisturbed velocity, U_∞, and a zero gradient for the pressure. At the outlet a zero gradient is imposed for the velocity and for the pressure. At the cylinder surface is imposed a zero velocity and zero gradient for the pressure. The time step used is equal to 0.001 s.

Simulations were made for an elastic cylinder with one degree of freedom for a number of cases where Re=200 and m^*=1.27. It is assumed that the cylinder is modeled as a spring-damper-mass system. The reduced velocity, U^*, ranges from 1 to 13, with 0.5 intervals. As mass, *m*, is the same for all cases, the stiffness of the spring, *k*, is changed from one simulation to another. The values of *k* span from 39.2 N/m (for U^*=1) to 0.23 N/m (for U^*=13), so as reduced velocity increases the stiffness of the system diminishes. The reduced velocity is inversely proportional to the frequency ratio, $f_n / f_s = \left(U^* St\right)^{-1}$, where f_s and St are the values for the static cylinder.

The damping ratio considered, $\zeta = 0.05$, is kept constant for all the simulations. So the damping coefficient, c, is changed from simulation to simulations to maintain the same m^* for different U^*. The combined mass-damping parameter, $m^*\zeta$, is 0.0635. The stability parameter, K_S, is 0.628.

3. RESULTS AND DISCUTION

3.1 Static cylinder with Re=200

The first study presented concerns the uniform flow past a static circular cylinder with Re=200. Figure 2a) presents the lift and drag coefficients, C_d and C_l, time series for the simulation from the initial instant of the simulation up to a dimensionless time, $\tau = tU_\infty / D$, of 150. The drag and lift coefficients are given by: $C_d = 2F_d / \rho D U_\infty^2$ and $C_l = 2F_l / \rho D U_\infty^2$, where F_d is the drag force (in the direction of the U_∞ vector) and F_l is the lift force (perpendicular to U_∞ vector).

As shown in Fig. 2a) both C_l and C_d settle to a regular sinusoidal regime after about 70τ. Figure 2b) presents the vorticity magnitude field at a given instant after the settling time period. The Strouhal number was found by applying a Fourier transform to the C_l time series after 70τ. Its value is presented in Tab. 1 along with values from other authors. Table 1 also presents the values of the mean value of C_d, C_{dmean}, and the root mean square of C_l, C_{lrms}.

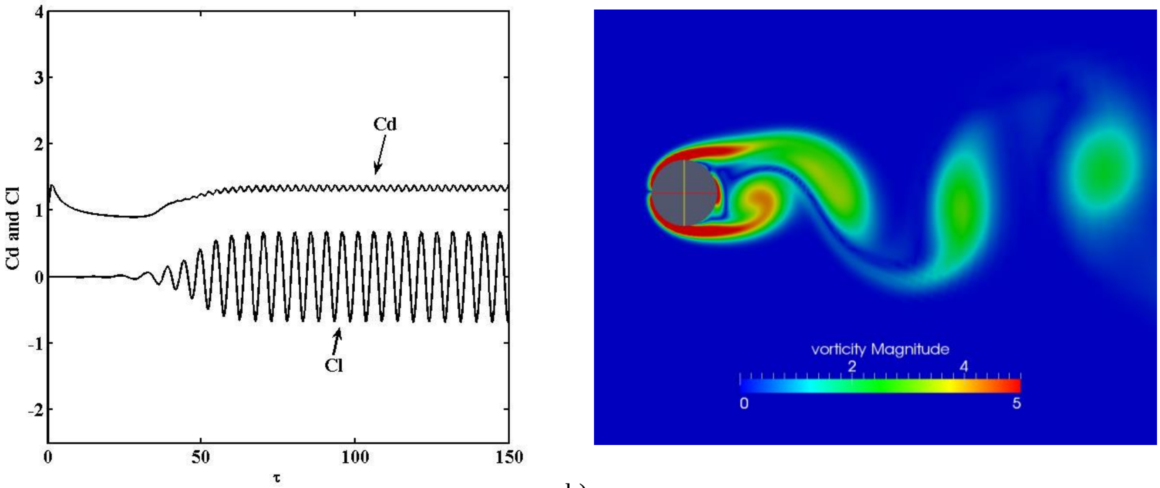

a) b)

Figure 2. Drag and lift coefficients, C_d and C_l, time series (a) and vorticity field (b) for a static cylinder at Re=200.

The selection of the domain dimensions is a common problem in numerical simulation of flow around cylinders. The results depend on the domain size due to the blockage effect, so the domain size and computational cost must be balanced to obtain the best results. Posdziech and Grundmann (2007) presented a study on the dependence of relevant variables with L_{ext} (defined in Fig. 1). Table 1 shows that for the L_{ext}/D considered in the present study the values obtained are in good agreement with those of the other authors.

3.2 Elastic cylinder with Re=200

Figure 3 presents the drag and lift coefficients time series together with the dimensionless cross-flow displacement, Y/D, time series for different reduced velocities, U^*, with and without damping. Figure 4a) presents the dimensionless peak-to-peak amplitude, Y_{max}/D, versus reduced velocity, U^*. Figure 4b) presents the dimensionless vortex shedding frequency, f/f_n, versus reduced velocity. Figures 5a) and 5b) present the mean drag, C_{dmean}, and the root mean square lift, C_{lrms}, coefficients versus reduced velocity.

When the natural frequency of the cylinder is larger than the vortex sheading frequency (higher values of f_n/f_s or lower values of U^*), the vortex sheading is similar to the one of the rigid cylinder, and the time series are similar. Up to U^*=2.5 (f_n/f_s=2.04) the time series are similar to the ones in Fig. 3a-b which are similar to Fig. 2a. The drag and lift coefficients and the cross-flow displacement increase slightly with U*, as it can be seen also by Y_{max}/D (Fig. 4a), by C_{Dmean} (Fig. 5a) and by C_{lrms} (Fig. 5b). The vortex shedding frequency, f, follows the static cylinder line (Fig. 4b).

Table 1. Strouhal number (*St*), root mean square of lift coefficient ($C_{l\mathrm{rms}}$) and mean drag coefficient ($C_{d\mathrm{mean}}$) for a static cylinder at Re=200.

Author	L_{ext}/D	*St*	$C_{d\mathrm{mean}}$	$C_{l\mathrm{rms}}$
Present results	50	0.1961	1.3326	0.4804
Posdziech and Grundmann (2007)	40	0.1962	1.3330	0.4794
Posdziech and Grundmann (2007)	200	0.1946	1.3158	0.4712
Didier (2012)	140	0.1950	1.3186	0.4712
Didier (2012)	500	0.1944	1.3132	0.4691
Didier and Parxotomo (2014) - Fluent	150	0.1942	1.3152	0.4708
Didier and Parxotomo (2014) - FullCReM	150	0.1947	1.3162	0.4703

As the reduced velocity increases (f_n/f_s decreases) the cylinder vibration starts to affect the vortex sheading, for U*=3 and 3.5 (Fig. 3c-f) a beating behavior appears and differences are visible between the solution with and without damping. This beating is a consequence of another frequency, resulting from a different vortex sheading pattern. The drag and lift coefficients and the cross-flow displacement increase significantly with U*.

At U*=4 the beating disappears, at U*=5 a phase shift occurs, and for higher values of U* the Y time series is in anti-phase with C_l.

As seen in Fig. 4a, from U*=3.5 to 8.5 Y_{max} experiences a regular decrease, and at U*=9 Y_{max} falls to a lower value that remains constant for higher values of U*.

As seen in Fig. 5a, from U*=5 to 8.5 C_{dmean} experiences a regular decrease to values inferior to the one of the static cylinder, and for higher values of U* remains almost constant.

As seen in Fig. 5b, from U*=3.5 to 4.5 C_{lrms} falls to a lower value inferior to the one of the static cylinder, from U*=4.5 to 8.5 C_{lrms} experiences an oscillation, and for higher values of U* increases slightly.

As seen in Fig. 4b, from U*=4.5 to 8.5 C_{lrms}, the dimensionless vortex shedding frequency is almost constant at a value of 1.1 (synchronization or lock-in), for values of U* lower that this interval the vortex shedding frequency is almost equal to the value of the static cylinder, for values higher than this interval the vortex shedding frequency is lower than the value of the static cylinder. The phase shift occurs in the lock-in region, corresponding to a frequency of oscillation near the natural frequency.

4. CONCLUSIONS

This paper presents the application of the numerical code OpenFOAM to the uniform flow past a cylinder that is static or allowed to move with 1 degree of freedom in the transverse direction to the flow. The Reynolds number is 200 for all simulations and the cylinder motion is described according to a mass-spring or a mass-spring-damper systems. The simulations were performed by solving the 2D Navier-Stokes equations.

In the simulation of the flow around the fixed cylinder, the drag and lift coefficients and Strouhal number, were calculated and compared with results from other authors. The results obtained are similar those of other authors, however it was noticed that the discretization and domain size are very important for the accuracy of the results.

In the simulations of the flow around the elastic cylinder (mass-spring or mass-spring-damper systems), the mass ratio is $m^* = 1.27$ and the combined mass-damping parameter is $m^*\zeta = 0.0635$. Drag and lift coefficients and the cylinder displacement were calculated for values of U* ranging from 1 to 13. The results obtained in this study were satisfactory and it is concluded that the OpenFOAM code is a reliable tool to solve problems with the VIV phenomenon.

As future work, this methodology will be applied to an elastic circular cylinder with one and two degrees of freedom and compared with experimental data. A more detailed study on the mesh dependency and domain size for a fixed cylinder will also be performed.

5. ACKNOWLEDGEMENTS

The authors acknowledge the support of the Strategic Plan for the Research & Development Unit in Mechanical and Industrial Engineering – UNIDEMI (UID/EMS/00667/2013).

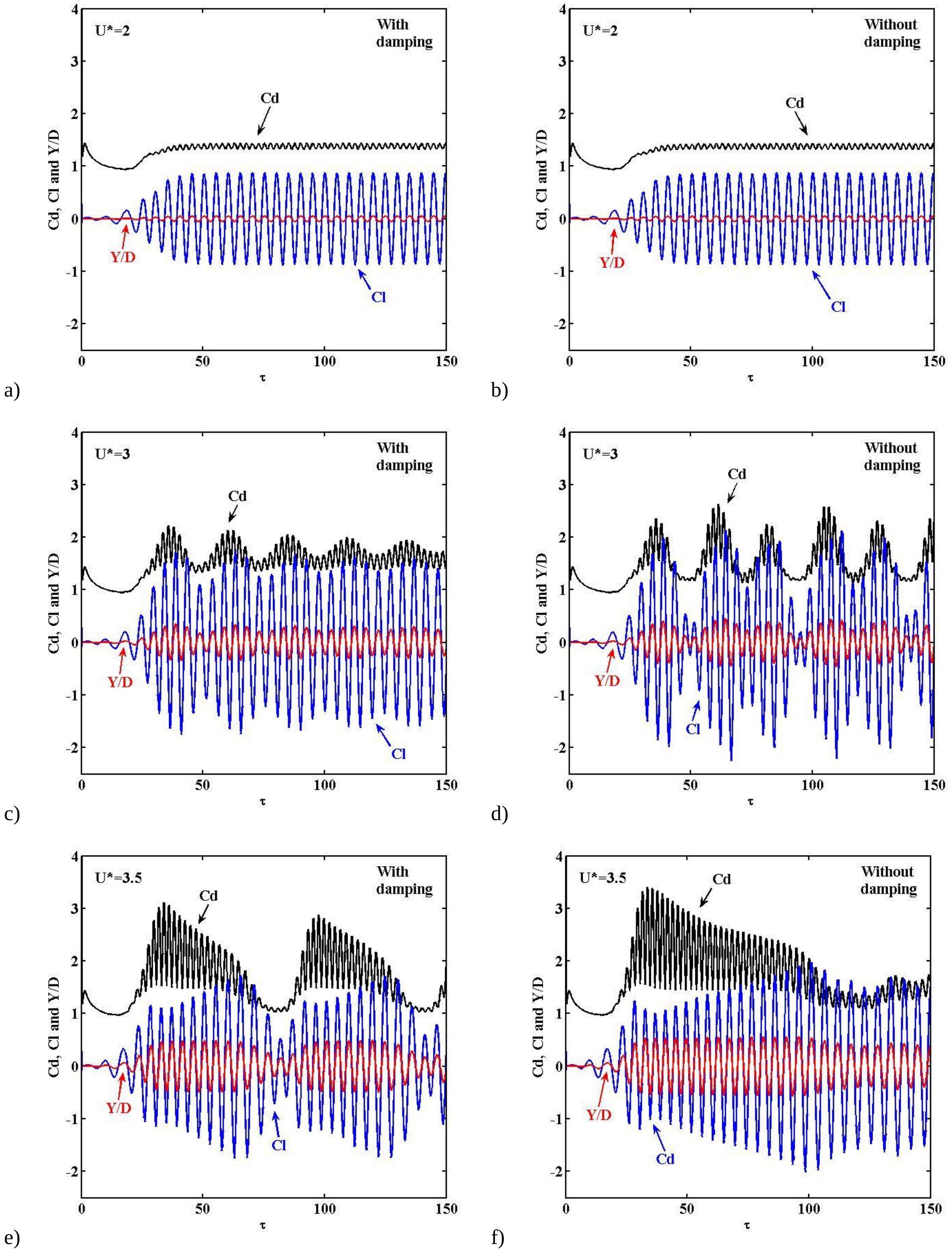

Figure 3. Drag and lift coefficients, C_d and C_l, and dimensionless cross-flow displacement, *Y/D*, time series for different reduced velocities, *U**, with and without damping for a static cylinder at *Re*=200.

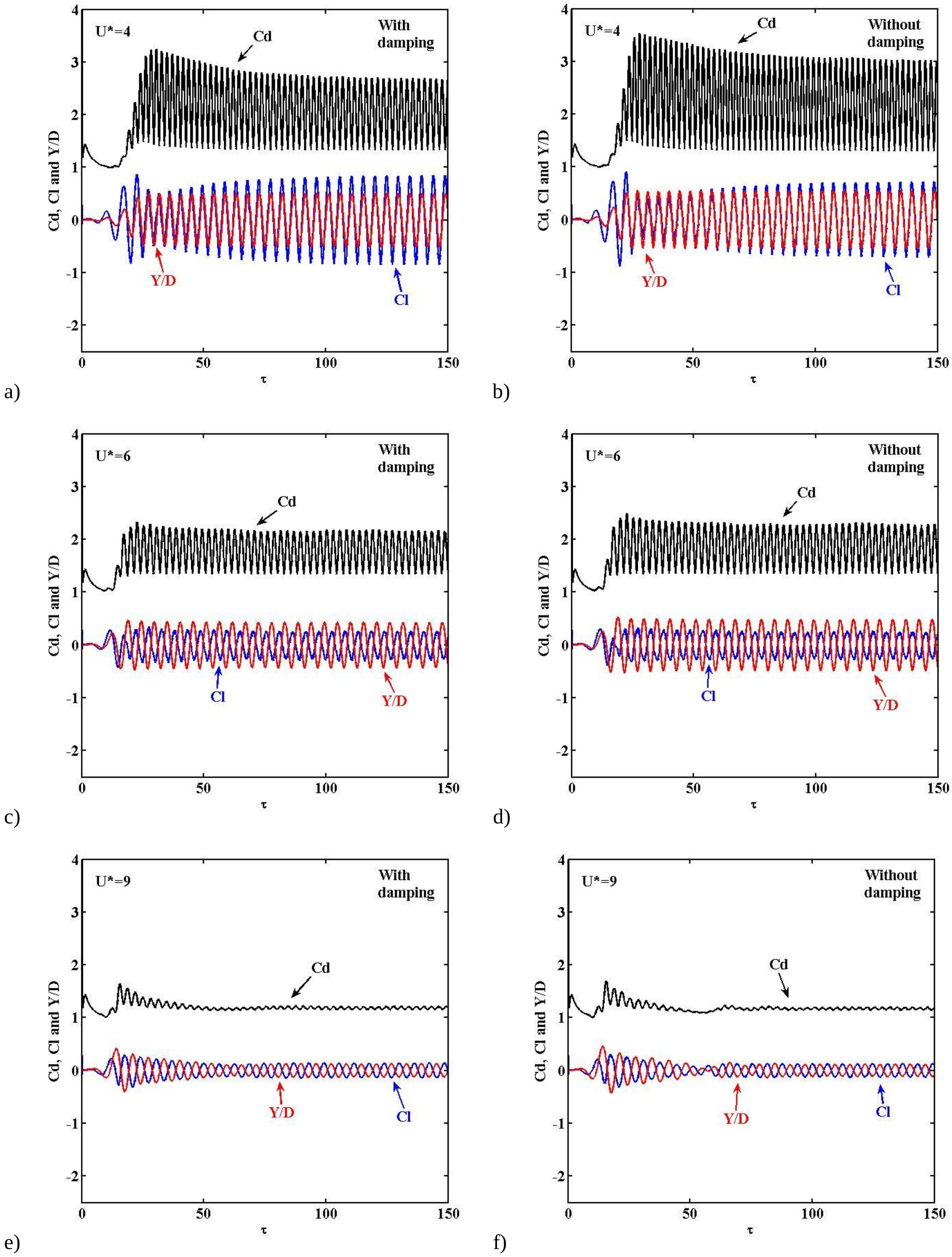

Figure 3. Drag and lift coefficients, C_d and C_l, and dimensionless cross-flow displacement, *Y/D*, time series for different reduced velocities, *U**, with and without damping for a static cylinder at *Re*=200 (continued).

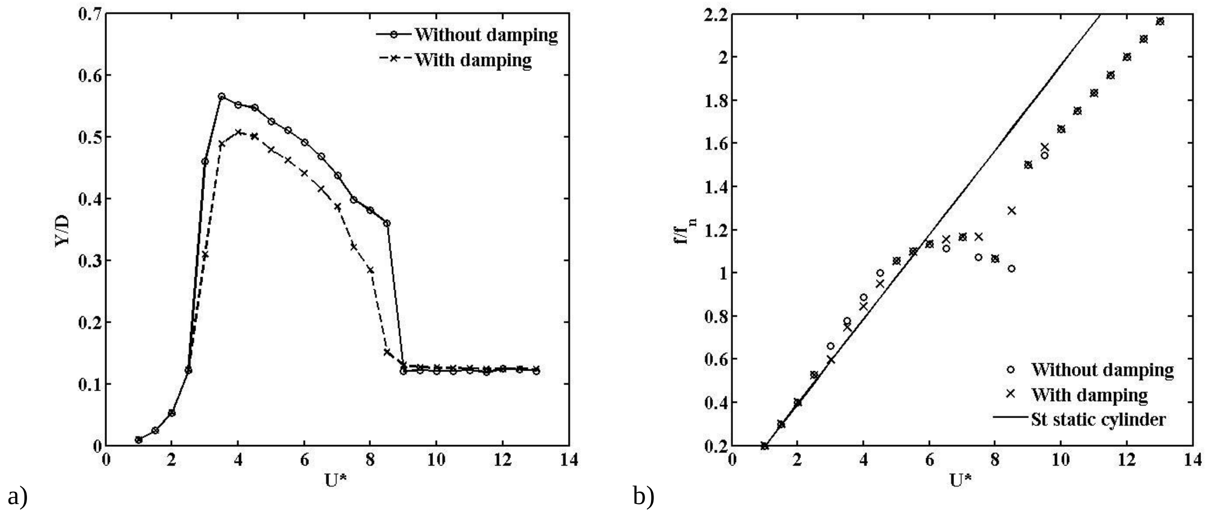

Figure 4. Dimensionless peak-to-peak amplitude, Y_{max}/D, versus reduced velocity, U^*, (a) and dimensionless vortex shedding frequency, f/f_n, versus reduced velocity (b) with and without dumping.

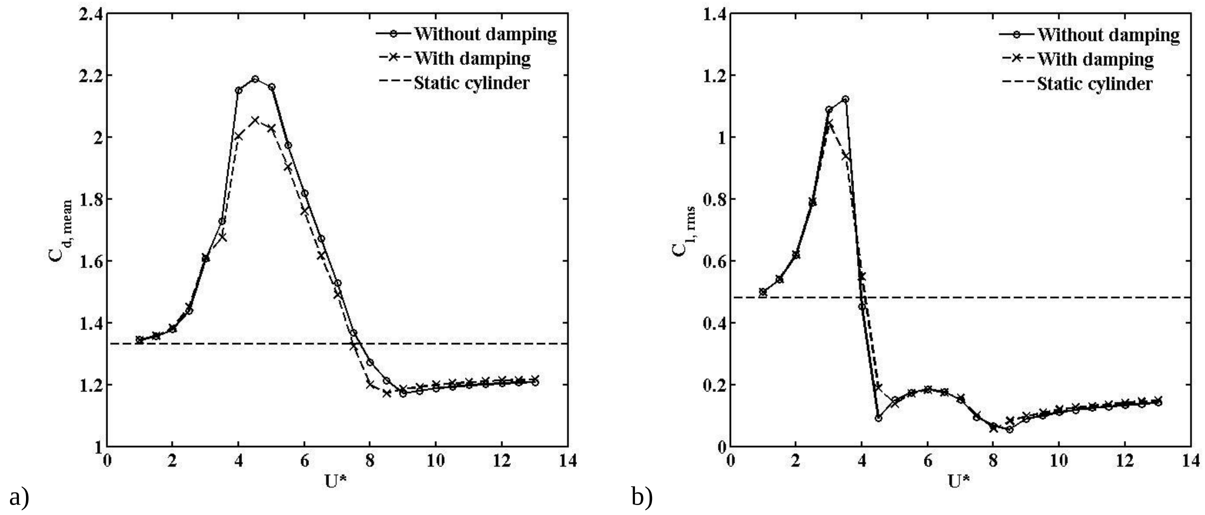

Figure 5. Mean drag, C_{Dmean}, (a) and root mean square lift, C_{Lrms}, (b) coefficients versus reduced velocity, U^*, with and without dumping.

6. REFERENCES

Blevins, R. D., 1977. *Flow-Induced Vibration*. Van Nostrand Reinhold Company Regional Offices, New York.

Didier, E., 2008. "Asymptotic convergence of fundamental quantities in numerical modeling of flow around a circular cylinder" (in portuguese). *Revista Iberoamericana de Ingeniería Mecánica*, Vol. 16, N. 1, pp 87-99.

Didier, E. and Parxotomo, D., 2014. "Force reduction in a circular cylinder using two small control cylinders in the wake" (in portuguese). *Revista Iberoamericana de Ingeniería Mecánica*, Vol. 18, N. 1, pp 23-45.

Fredsϕe, J. and Sumer, B.M., 1997. *Hydrodynamics around cylindrical structures*. World Scientific Publishing Co. Pte. Ltd., Singapore, vol. 12.

Geuzaine C. and Remacle J.-F, 2009. "Gmsh: a three-dimensional finite element mesh generator with built-in pre- and post-processing facilities". *International Journal for Numerical Methods in Engineering*, Vol. 79, N. 11, pp. 1309-1331.

Jasak, H. and Tupovic, Z, 2010. "Dynamic Mesh Handling in OpenFOAM Applied to Fluid-Structure Interaction Simulations". In *Proceedings of the V European Conference on Computational Fluid Dynamics - ECCOMAS CFD 2010*. Lisbon, Portugal.

Li, T., Zhang, J., Zhang, W., and Zhu, M., 2009. "Vortex-Induced Vibration Characteristics of an Elastic Circular Cylinder". *World Academy of Science, Engineering and Technology*, Vol. 3, N. 12, pp. 50 - 59.

OpenFOAM, 2013. "The Open Source CFD Tollbox – User Guide v.2.2.2". 1 Nov.2013. <http://www.openfoam.com>.

Posdziech, O. and Grundmann R., 2007. "A systematic approach to the numerical calculation of fundamental quantities of the two-dimensional flow over a circular cylinder". *Journal of Fluids and Structures*, Vol. 23, pp. 479-499.

Williamson and Govardhan, 2004. "Vortex-Induced Vibrations". *Annu. Rev. Fluid Mech.*. Vol. 36, pp. 413–55.

Zdravkovich, M. M., 1997. *Flow around circular cylinder, Volume 1: Fundamentals*, Oxford University Press Inc, New York.

Zhou, C.Y., Sorm, C., Lam, K., 1999. "Vortex induced vibrations of an elastic circular cylinder", J. Fluids Struct. Vol. 13, pp. 165-189.

7. RESPONSIBILITY NOTICE

The authors are the only responsible for the printed material included in this paper.